

Supplementary Information

***In silico* design of supramolecules from their precursors: odd-even effects in cage-forming reactions**

Kim E. Jelfs, Edward G. B. Eden, Jamie L. Culshaw, Stephen Shakespeare, Edward O. Pyzer-Knapp, Hugh P. G. Thompson, John Bacsá, Graeme M. Day, Dave J. Adams, Andrew I. Cooper*

* To whom correspondence should be addressed. E-mail: aicooper@liv.ac.uk

This document includes:

1. Experimental details.
2. Computational details and validation.
3. Computational results.
4. References.

Figures S1 to S10.

Tables S1 to S4.

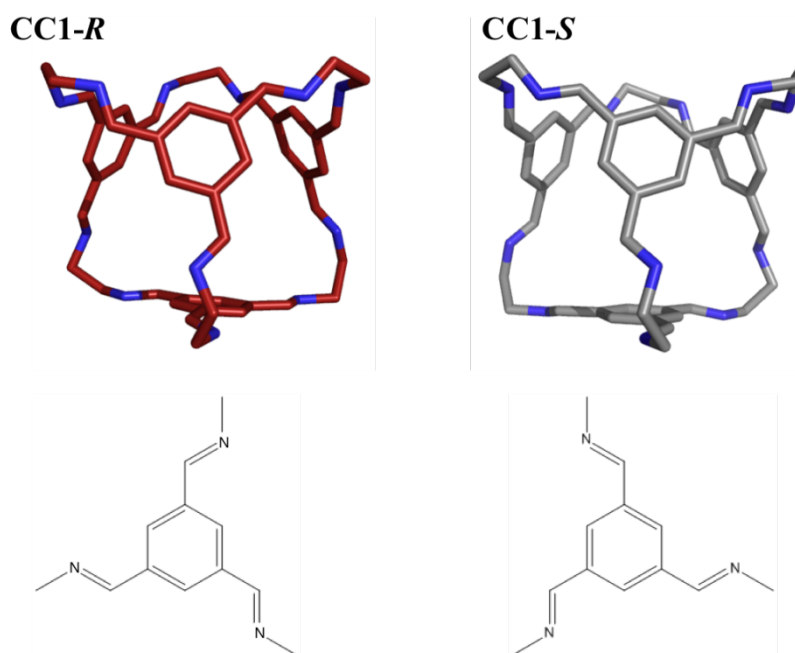


Figure S1. The observed tetrahedral conformer of **CC1**, showing the two possible helical enantiomers. The *R* enantiomer of this conformer is shown in red, the *S* enantiomer in gray; nitrogens are shown in blue. Hydrogen atoms are omitted for clarity. The bottom row shows a single aryl face of each conformer.

1. Experimental details

The synthesis and characterization for **CC1** is described elsewhere.¹

1.1. Synthesis of CC-propane. To a cooled (0 °C) solution of propane-1,3-diamine (54.4 mg, 1.58 eq) and DMF (1 drop as internal NMR standard) in DCM (50 mL) was added by syringe pump a solution of benzene-1,3,5-tricarbaldehyde (75.2 mg, 1.0 eq) in DCM (40 mL) over 24 h. The resultant mixture was allowed to warm to room temperature and maintained for 72 h to afford a turbid solution. Completion of the reaction was confirmed by ¹H NMR. Mass spectrometry (MS) and NMR data were obtained directly by *in situ* sampling of the reaction mixtures. All attempts at isolating the product resulted in significant amounts of insoluble materials being formed. Yields were therefore calculated by use of an internal standard (DMF), which was added to the solution of the aldehyde in DCM prior to addition of the amine. Integrals associated with the aldehyde (-CH=O, 10.22 ppm), before addition, and the imine (-CH=N, 8.14 and 8.22 ppm for **CC-propane** and **CC-butane** respectively), at reaction completion, were normalized against the standard to determine the proportion of cage in solution once the reaction was complete. Insoluble material was assumed not to be product. The *in situ* NMR showed clean, single product with the expected [2+3] stoichiometry, with integration relative to DMF demonstrating a yield of 24 %. The remainder of the product was an insoluble polymer. *m/z* = 439.3 (M+H⁺); ¹H NMR: (400 MHz, CDCl₃) δ ppm 2.41 (quin, J = 5.0 Hz, 2 H) 3.89 (t, J = 5.0 Hz, 4 H) 7.79 (s, 3 H) 8.14 (s, 3 H).

Attempts at purifying the material by filtration resulted in the material becoming insoluble on isolation. Concentrating the material and then slowly evaporating the solvent also resulted in insoluble material being formed.

We also attempted to adjust the solvent environment post-synthesis: To a colorless, cooled (0 °C) solution of 1,3,5-triformylbenzene (450 mg) in dichloromethane (100 mL) was added, under nitrogen, a solution of 1,3-propanediamine (309 mg) in dichloromethane (130 mL) over 18 h to afford a colorless solution. The resultant mixture was maintained for 120 h. The reaction mixture was concentrated under reduced pressure (1/2 volume) and diluted with methanol, this procedure being repeated three times to afford a clear, colorless solution in which was suspended an off-white solid. This material was found to be insoluble in chloroform after isolation by filtration.

Finally, we attempted to isolate the material by slow crystallisation. Here, samples (prepared by taking the solutions of DMF-internal-standard experiments) were dissolved in DCM, filtered, and placed in 3 dram vials. These were placed into 10 dram vials, to which was subsequently added MeOH, EtOAc, CHCl₃, IPA, Et₂O, iPr₂O, EtOH, acetone, THF, hexane, MeCN or Toluene: The table below shows the results of these attempts at isolation.

Solvent	After 3 days	Solubility in CDCl ₃
MeOH	Film	No
EtOAc	Ppt	No
CHCl ₃	Clear	-
IPA	Film	No
Et ₂ O	Ppt	No
iPr ₂ O	Turbid	-
EtOH	No	No
Acetone	Clear	-
THF	Clear	-
Hexane	Film	No
MeCN	Film	No
Toluene	Clear	-

Solids, where formed, were separated by filtration. None of these solids were found to dissolve in chloroform.

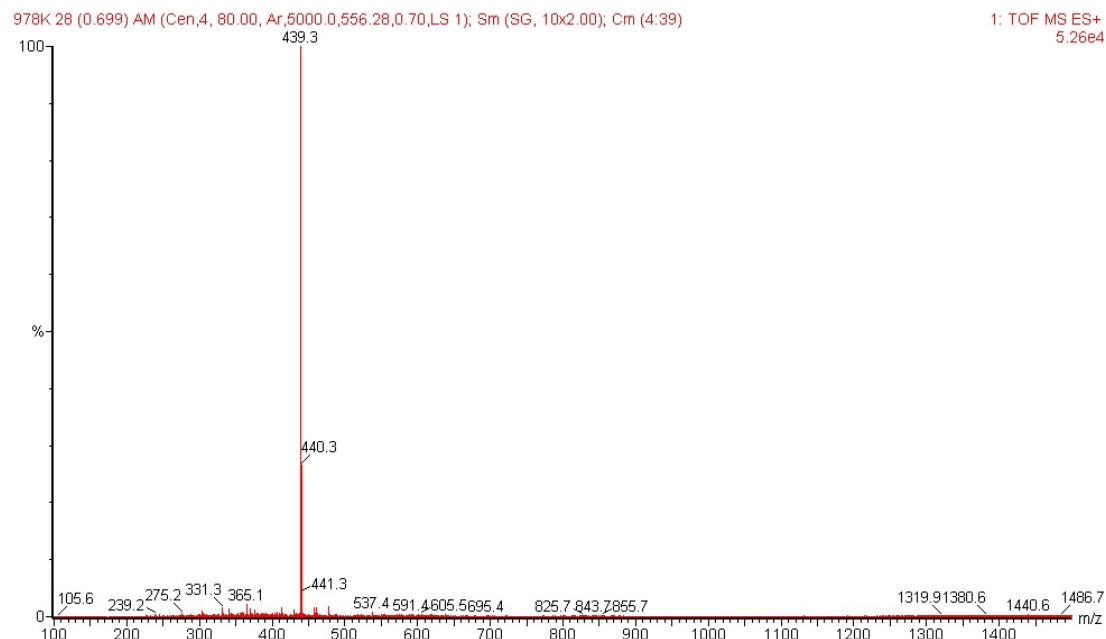


Figure S2. Mass spectrometry data for [2+3] cage **CC-propane**.

1.2. Synthesis of CC-butane. To a cooled (0 °C) solution of butane-1,4-diamine (64.9 mg, 1.58 eq) and DMF (1 drop) in DCM (50 mL) was added dropwise a solution of benzene-1,3,5-tricarbaldehyde (76.3 mg, 1.0 eq) in DCM (40 mL) over 12 h. The resultant mixture was allowed to warm to room temperature and maintained for 72 h to afford a turbid solution. Completion of the reaction was confirmed by ^1H NMR. Again, MS and NMR data were obtained directly from reaction mixtures. The *in situ* NMR showed a clean, single product with the expected [2+3] stoichiometry, with integration relative to DMF demonstrating a yield of 27 % (using the imine peak at 8.23 ppm). The remainder of the product was insoluble. As for the **CC-propane**, all attempts at isolating the material resulted in insoluble material being collected. m/z = 961.6 (M+H $^+$); ^1H NMR: (400 MHz, CDCl_3) δ ppm 1.60 (m, 12 H) 3.63 (t, J =6.67 Hz, 12 H) 8.01 (s, 6 H) 8.22 (s, 6 H).

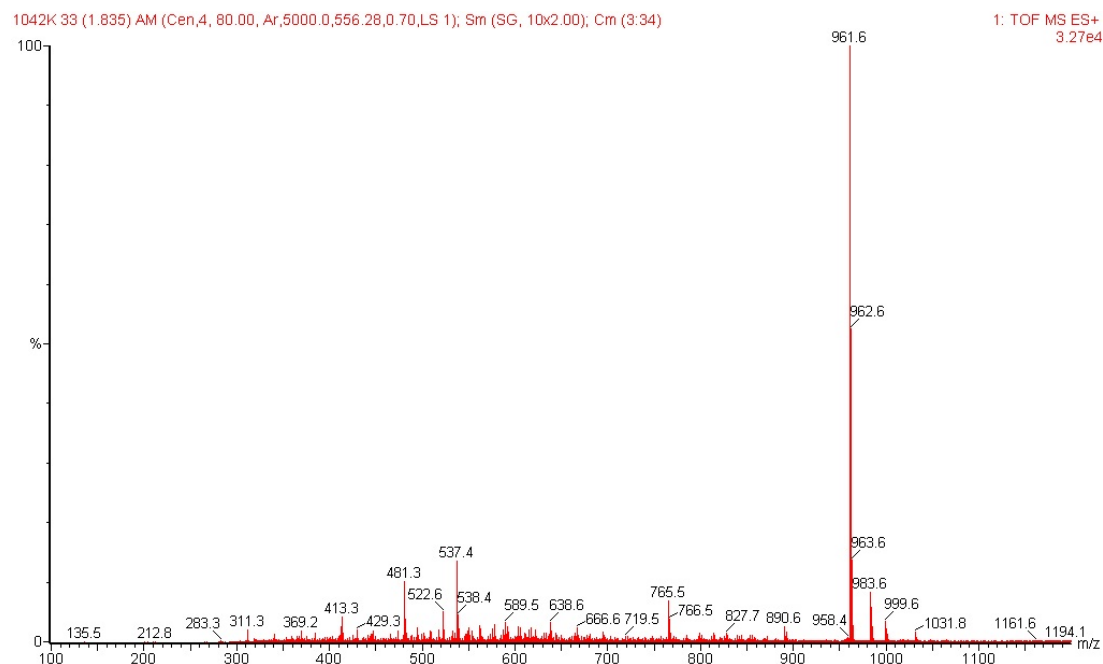


Figure S3. Mass spectrometry data for **CC-butane**.

1.3. Synthesis of CC-pentane. To a cooled (0 °C) solution of pentane-1,5-diamine (425 mg, 1.5 eq) in DCM (50 mL) was added dropwise a solution of benzene-1,3,5-tricarbaldehyde (450 mg, 1.0 eq) in DCM (40 mL) over 6 h. The resultant mixture was allowed to warm to room temperature and maintained for 120 h to afford a clear, light-yellow solution. Solvents were removed under reduced pressure to afford a pale yellow solid (875 mg, 100 %). Crystals were then grown by immediately dissolving the cage in dichloromethane, before layering with methanol in a glass vial, and leaving the solutions to slowly diffuse which induced the growth of crystals on the sides of the vial over several days. $m/z = 523.5$ ($M+H^+$, 100%); 1H NMR: (400 MHz, $CDCl_3$) δ ppm 0.88 (m, 1 H) 1.77 (tt, $J = 8.2, 5.2$ Hz, 2 H) 3.61 (t, $J = 5.2$ Hz, 2 H) 7.86 (s, 1 H) 8.09 (s, 1 H).

On attempting to re-dissolve the material from which the sample was taken for analysis, re-dissolution is not complete in chloroform. Hence, the material is stable in solution, but not upon isolation in the solid state.

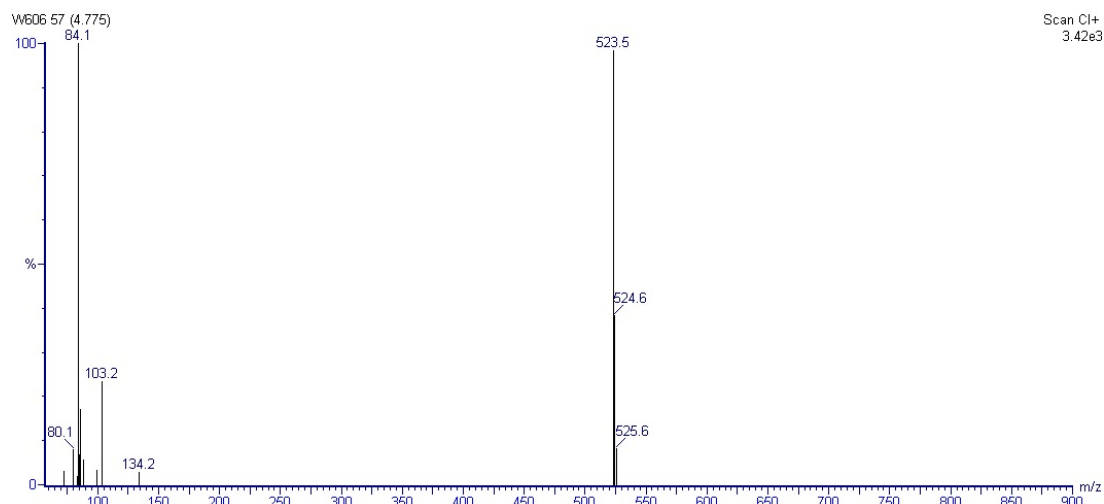


Figure S4. Mass data spectrometry for **CC-pentane**.

1.4 Single Crystal X-ray Diffraction.

Single crystal X-ray data for **CC-pentane** was collected on a Bruker APEX diffractometer with 1.5 kW graphite monochromated Mo radiation ($\lambda = 0.7107 \text{ \AA}$). The detector to crystal distance was 60 mm and the temperature of the crystal was maintained at 173 K throughout the data collection. The crystal diffracted to a maximum theta angle of 25.35° . Total reflections collected, 16746, independent reflections 6779 unique ($R(\text{int}) = 0.0510$); parameters, 352; $R1 = 0.0998$; $wR2 = 0.2020$; density, $= 1.122 \text{ g cm}^{-3}$. The frames were integrated with the SAINT v7.68a (Bruker, 2009).² A multi-scan absorption correction was carried out using the program SADABS V2008-1 (Bruker, 2008).³ The structures were solved and refined with X-SEED,⁴ a graphical interface to SHELX (Sheldrick, 2008).⁵ The cage structures refined well but the electron density corresponding to solvent molecules was diffuse and, due to the high symmetry, could not be modelled using disordered solvent molecules. Instead, an approximate number of methanol molecules was determined using PLATON/SQUEEZE⁶ and their contribution subtracted to the X-ray diffraction data. This corresponds to either 7 methanol molecules, or 6 methanol molecules plus 2 water molecules. Hydrogen atoms were placed in geometrically idealized positions. In the final cycles of refinement, all non-hydrogen atoms were refined anisotropically and hydrogen atoms were refined with their distances and thermal parameters constrained.

The crystallographic data for the **CC-pentane** methanol solvate is attached as additional supporting information.

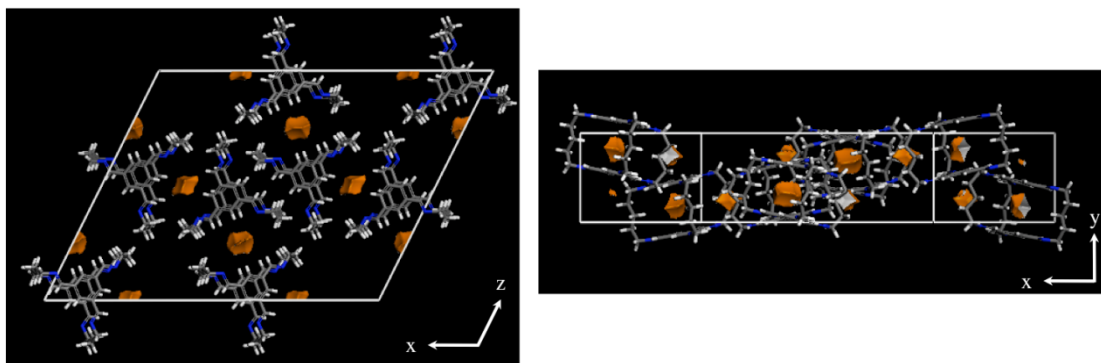


Figure S5. Single crystal X-ray structure of the **CC-pentane** methanol solvate, viewed down the y axis (left) and down the z axis (right). The solvent was removed using PLATON/SQUEEZE and is not shown. The structure contains only isolated voids (shown in orange), as estimated from a solvent accessible surface calculated using a probe radius of 1.82 Å (equivalent to the radius of a nitrogen molecule⁷) in Materials Studio 5.0 (Accelrys Inc.). Carbons are shown in grey, nitrogens in blue, and hydrogens in white.

2. Computational details

2.1. Conformer searching method

We used the MacroModel (version 9.9, Schrödinger, LLC, New York, NY, 2011) conformer searching tool to search for all the low-energy conformers for each structure. We first validated that this approach finds known alternative conformers for published organic cage systems, and that it gives reasonable relative energies by examining case studies from other imine cages that we have reported previously (see Section 2.4). The procedure uses a low-mode (LMOD)⁸ sampling approach which follows the low frequency eigenvectors of the molecule. This has been used previously to examine cyclic alkanes. We used 50,000 search steps for [2+3] molecules and 500,000 steps for the larger [4+6] molecules. The maximum and minimum move distances were 3 and 12 Å, with all structures within an energy window of 50 kJ mol⁻¹ of the lowest energy structure being retained. This number of steps was chosen because repeats of the calculations found no new low energy structures, with each conformation sampled multiple times within an individual run. For geometry optimization, the convergence criterion was a remaining RMS force of 0.05 kJ mol⁻¹ Å⁻¹. These cages can often exist in two alternative enantiomers (*R* and *S*) related by helical chirality:⁹ since these have equivalent energies, we only retained one mirror-image conformer. We used an automated procedure (Section 2.5) to check for conformations with an internal ‘pore’, defined here as a spherical space with a radius of >2.5 Å. If none was found, then we repeated the search with an additional 250,000 steps and a search window of 500 kJ mol⁻¹ in order to see whether any structures with an internal void could be found lying higher in energy.

We applied a final refinement of the structures and energies by optimizing the resulting molecular structures with DFT-D3 calculations performed in CP2K¹⁰ with the PBE functional,¹¹ TZVP-MOLOPT basis sets,¹² GTH-type pseudopotential,¹³ a plane wave grid cutoff of 400 Ry, a cubic box of length 50 Å, and the Grimme-D3 dispersion correction.¹⁴ This procedure was applied to any structure within 25 kJ mol⁻¹ of the lowest energy conformer, which we determined as the maximum error in the

energy difference between structures for the OPLS force field (see Section 2.3). We have previously used this DFT setup to reliably reproduce the structure and energetics of porous imine cages in both the solid state^{3,15} and as single molecules and dimer pairs.^{4,16}

2.2. Performance of OPLS forcefield for porous organic imine cages

Many of the commonly available, transferable forcefields perform poorly at reproducing the structures of porous organic imine cages, either because they do not contain the relevant parameters for, or are poorly parameterized for, the angles and torsions around the imine bond. Hence, optimization of the cage molecules by these forcefields, such as UFF^{5,17} and PCFF^{6,18}, severely distorts the tetrahedral structure of the cages upon minimization. However, upon testing the OPLS all-atom forcefield (Optimized Potentials for Liquid Simulations),^{7,19} it performed very well at reproducing both the molecular structures and molecular energies of a range of known imine cages. The OPLS forcefield was developed for organic and biomolecular systems, with the focus on fitting being the energetics of conformers, intermolecular gas phase energies and testing against thermodynamic properties of pure organic liquids, particularly heats of vaporization and densities.

We took single cage molecules from the single crystal X-ray structures of several published imine cages that were also formed using 1,3,5-triformyl benzene: **CC2** (1,2-propylenediamine)^{8,20}, **CC3** (1,2-diaminocyclohexane)^{10,20}, **CC4** (1,2-diaminocyclopentane),^{11,21} and **CC9** (1,2-diphenylethylenediamine)^{12,22}. All of these cages have a [4+6] ratio of aldehyde to amine precursors. We then geometry optimized these isolated cage molecules using OPLS-2005 using MacroModel, part of the Schrodinger software package (MacroModel, version 9.9, Schrödinger, LLC, New York, NY, 2011), until the remaining force was less than 0.05 kJ Å⁻¹ mol⁻¹. Figure S6 shows overlays of the molecular structure from the X-ray data and the OPLS minimized structures. The structures are very well reproduced, in particular the core cage structures. The root mean square displacements, including hydrogens, are 0.072 Å (**CC3**), 0.142 Å (**CC4**) and 0.206 Å (**CC9**). The **CC2** structure cannot be compared in this quantitative fashion due to the disorder in the methyl positions across the two possible vertex positions in the single crystal X-ray diffraction structure. There is some small difference in the cyclopentane vertices of **CC4**, but these are disordered in the crystal structure in any case. There are also some differences in the phenyl group torsions on the vertices of **CC9**, where there is presumably facile rotation and a flat potential energy surface. The latter is not considered to be a problem because this type of fragment is not present in the new alkanediamine cage molecules examined here, although this could become an important consideration in building a more generic methodology. Finally, from previous DFT+D calculations on the molecular structures, the two lowest energy **CC1** conformers (with T and C₃ symmetry, respectively) were found to lie 13 kJ mol⁻¹ apart^{9,13}. Geometry optimized structures of these two molecules in OPLS were found to lie 15 kJ mol⁻¹ apart, a good agreement with this DFT value. Taken in combination, these results gave us confidence that OPLS could be used for the reliable description of both the 3-D structures and the relative energies of the new organic cages reported in the main text.

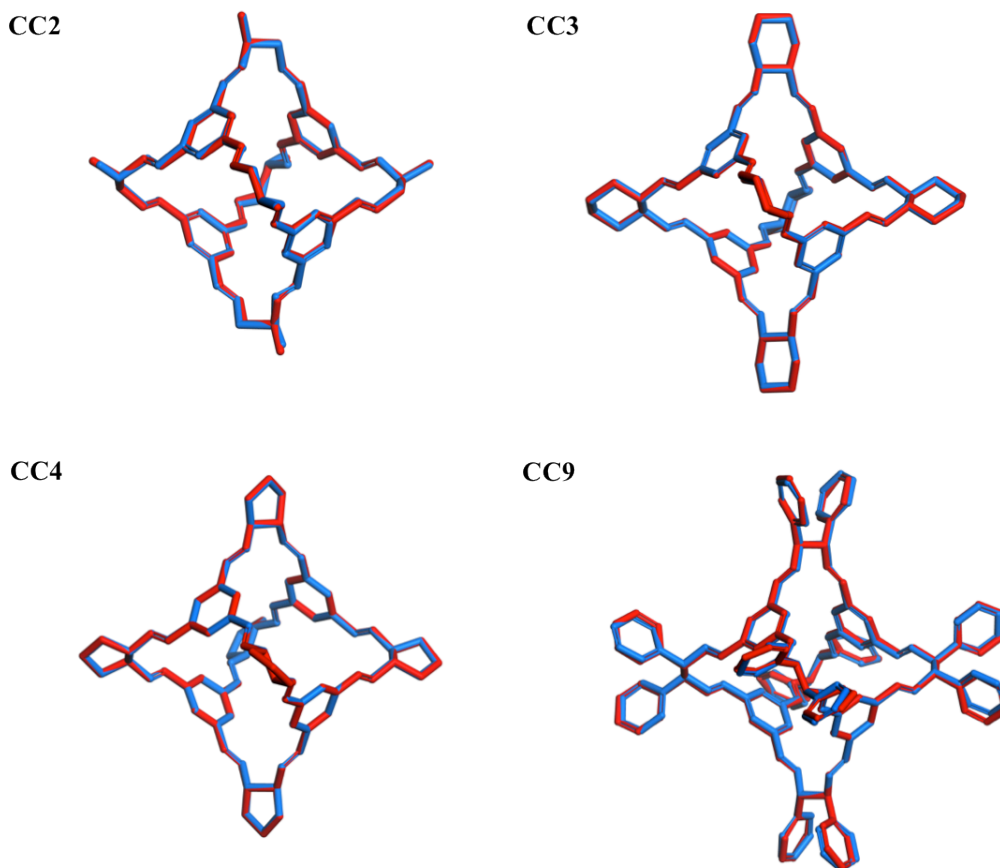


Figure S6. Overlays of the molecular cage structures taken from single crystal X-ray structures (blue) and the OPLS-minimized structures (red). Hydrogens are not shown.

2.3. Relative energies of OPLS and DFT

In order to select which band of low-energy structures from the OPLS conformer search to refine using PBE/TZVP-MOLOPT DFT+D3 calculations, it was first necessary to establish a confidence level in the forcefield. By determining the maximum magnitude of the energetic reordering of the structures from OPLS to DFT calculations, it can be ensured that the ‘true’ lowest energy structure is not missed because it lies too far above the lowest energy OPLS structure. To do this, the energies of the [2+3] and [4+6] molecules formed from 1,3,5-triformylbenzene (TFB) and 1,5-diaminopentane were compared from both OPLS and DFT calculations. The results are shown in Figure S6 and Tables S1 and S2. These data show that there is some reordering of the relative energies of the structures, with the absolute numbers being fairly small. For the [2+3] structures, the maximum change in relative energy was found to be 8.2 kJ mol^{-1} , and for the [4+6] structures, the maximum change was 11.4 kJ mol^{-1} . On this basis, the confidence level in the forcefield was determined to be 20 kJ mol^{-1} . Hence, for all systems, all structures from the OPLS conformer search that were within 20 kJ mol^{-1} of the lowest energy structure were reoptimized in DFT calculations in order to find the final, lowest energy conformer.

OPLS ranking	OPLS E_{rel} (kJ mol ⁻¹)	DFT ranking	DFT E_{rel} (kJ mol ⁻¹)	Difference (OPLS-DFT)
1	0	4	0	0
2	0.3	1	-7.9	-8.2
~3	2.7	2	-1.5	-4.2
~3	2.7	3	-1.4	-4.1
5	3.7	5	10.0	6.3

Table S1. Reordering of the structures of [2+3] molecules formed from TFB and 1,5-diaminopentane based on OPLS and DFT calculations.

OPLS ranking	OPLS E_{rel} (kJ mol ⁻¹)	DFT ranking	DFT E_{rel} (kJ mol ⁻¹)	Difference (OPLS-DFT)
1	0	5	0	0
2	2.1	1	-8.7	-10.8
3	3.0	4	-1.8	-4.8
4	3.5	2	-7.9	-11.4
5	3.9	3	-2.4	-6.3

Table S2. Reordering of the structures of [4+6] molecules formed from TFB and 1,5-diaminopentane based on OPLS and DFT calculations.

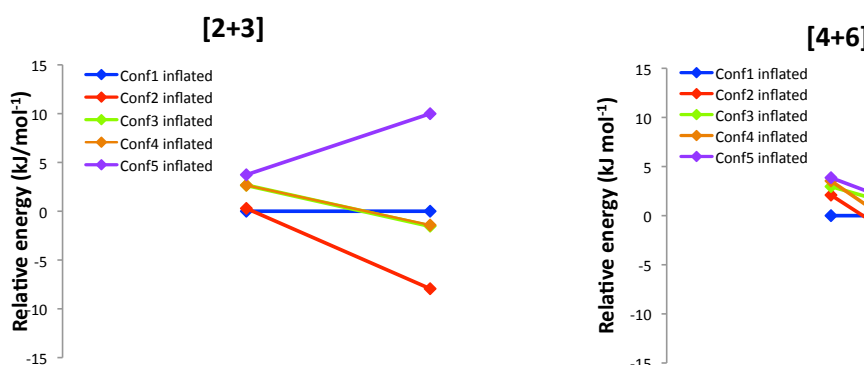


Figure S7. Reordering of the structures of [2+3] (left) and [4+6] (right) molecules formed from TFB and 1,5-diaminopentane from the OPLS energies and the PBE/TZVP-MOLOPT DFT+D3 energies. The energies are relative to the lowest energy conformer. The first points (on the left) are for OPLS, and the second points (to the right) are the DFT results.

2.4. Validation of conformer searching approach for porous organic cages

To validate the conformer searching procedure, several test case studies were identified, based on porous imine cages that have been reported previously. These test cases were:

- CC1** – there are two alternative T symmetry [4+6] cage molecules (enantiomers labeled *R* and *S* have helical chirality); these enantiomers, of course, have the same energy. There is an additional C₃ conformer that lies by ~13 kJ mol⁻¹ higher in energy.^{9,14}
- CC5** – there are two alternative T symmetry [4+6] cage molecules (*R* and *S* enantiomers, again isoenergetic); the lowest energy structure is expected to be

shape-persistent with a cavity, as exemplified by the highly porous nature of the bulk material for this cage.¹⁵

- iii) **CC7** – this is a large [8+12] cage molecule with a shape (in its solvate form) of a rhombicuboctahedral capsule, and a lower energy “collapsed” structure that lacks a permanent internal cavity, demonstrating that this cage, unlike **CC1** and **CC5**, is not shape persistent.²³

The conformer searching procedure outlined in the main text was carried out on structural models built from the relevant precursors (that is, not taken from single crystal X-ray diffraction data) in order to replicate our approach for the new molecules synthesized in this study, and to reflect the procedure that would be used for a hypothetical molecule that has not yet been synthesized. For these systems, only 15,000 steps were used in the conformer searching procedure. In brief, the results were as follows:

- i) For **CC1**, both of the tetrahedral enantiomers were found with the same energy (to within a fraction of a kJ mol^{-1}). In addition, another conformer was found with C_3 symmetry, where some of the $C_{\text{arene}}-C_{\text{arene}}-C_{\text{imine}}-N_{\text{imine}}$ torsions were flipped by 180° , which lay 13 kJ mol^{-1} higher in energy than the T conformers as calculated in OPLS. Both conformers were excellent matches with the relevant single crystal X-ray diffraction structures, and no lower-lying ‘collapsed’ structures were found, validating the known shape-persistence for **CC1**.
- ii) For **CC5**, the tetrahedral enantiomers were again found as the lowest energy structures, with the next conformer lying 15 kJ mol^{-1} higher in energy; this had a similar structure, with small rotations of the phenyl groups of the triphenylamine cage face. Again, this molecule was correctly determined to be shape-persistent and no low energy “collapsed” structures were found.
- iii) For **CC7**, the lowest energy conformer was found to be a collapsed structure with no internal cavity. More than 100 kJ mol^{-1} higher in energy (by OPLS) was found the rhombicuboctahedral capsule structure, which was observed in single X-ray crystal diffraction data for the solvated molecule. This is in agreement with the observed lack of shape-persistence for this larger cage, which collapses upon desolvation.

In summary, this conformational searching approach with OPLS successfully reproduces the desired structures, relative energies, and experimental shape-persistence (or lack of) for all three case studies.

2.5 Identifying conformations that contain an internal void: screening for shape-persistence

In order to automatically determine whether the various conformations found during the conformer searches for [4+6] molecules contained an internal void, we wrote a PERL script to determine the largest sphere that could fit within the center of the cage. First, the center of mass of each molecule was calculated, and then the shortest distance between this center of mass and any atom of the molecule was determined. This distance, minus the van der Waals radius of the atom ($C = 1.7 \text{ \AA}$, $H = 1.2 \text{ \AA}$, and $N = 1.55 \text{ \AA}$), was then defined as being the radius of the largest sphere that can fit

within the cage molecule. A molecule was then deemed to have an internal void if this radius was greater than 2.5 Å. This is equivalent to the cage molecule being able to encapsulate small guests such as H₂, N₂, CO₂, Xe, and common organic solvents.

The measured void radius for **CC1** here is 2.76 Å (Table S4), and this cage is known to encapsulate solvents such as dichloromethane and ethylacetate²⁴. Hence, since all the “inflated” conformations for the other cage molecules studied here have a void larger than this, it seems reasonable to assume that the solvents used here (methanol, DCM, ethyl acetate, ethanol and chloroform) are able to act as scaffolds for any of these structures.

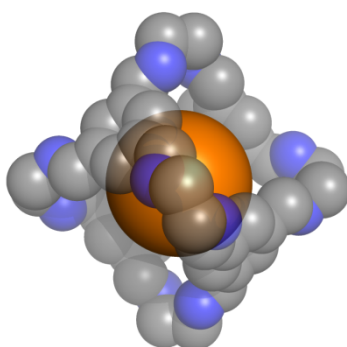


Figure S8. The largest sphere (in orange) that can fit within the internal void of the **CC1** molecule. **CC1** is shown with a space filling representation, omitting hydrogens, with transparency to show the void sphere.

3. Computational results

3.1. Structures and energies of low energy conformers for alkane cages

Alkane diamine	[2+3]	[4+6]	Collapsed [4+6]
1,2 ethane	0	-61 , -46	n/a
1,3 propane	0	+21	-6
1,4 butane	0, +2	-37 , -35, -30	-56
1,5 pentane	0 , +6, +8	+48, +54	-20

Table S3. Relative energies of the low energy conformers, expressed per [2+3] unit, from DFT+D3 calculations for [2+3] and [4+6] precursor combinations. The lowest energy conformer for each case is highlighted in **bold**. The right hand column gives the relative energy for the lowest energy conformer found with no internal cavity, if any.

3.2. Void sizes

Alkane diamine	[2+3]	[4+6]	Collapsed [4+6]
1,2 ethane	0.00	2.76	n/a
1,3 propane	0.65	4.39	0.00
1,4 butane	0.52	3.97	0.00
1,5 pentane	1.32	5.42	0.06

Table S4. Radius of the spherical internal void (Å) of the lowest energy conformation for each precursor combination. All [4+6] combinations can accommodate solvent, whereas, with the possible exception of the 1,5-pentane system, the [2+3] cages are unlikely to be able to accommodate solvent guests.

3.2. Predicted structures

We include the Cartesian coordinates for the predicted **CC-propane** and **CC-butane** molecular structures, for reference with any future, solved structures from experiment. The relevant cif files can also be supplied upon request.

CC-propane:

N	23.1302014743	22.0767429329	21.9932156620
C	23.3336112351	21.0332672891	21.0037001030
C	24.5538408211	21.3144546998	20.1102832217
C	25.9235629668	21.0930428497	20.7742209143
N	26.2468721219	22.1467296645	21.7200251792
H	22.4410557567	21.0166326207	20.3550899999
H	23.4275188679	20.0261328224	21.4642518973
H	24.4967376848	22.3481324962	19.7376573755
H	24.4911143506	20.6479197167	19.2354107435
H	26.6886463641	21.1167478597	19.9796803269

H	25.9571711166	20.0835921734	21.2382333150
N	23.6991510515	21.5450520007	28.3741346589
C	24.0956217059	21.2410542464	29.7385754019
C	25.4244249318	20.4678911736	29.7984283781
C	26.6876657225	21.2983488912	29.5155554017
N	26.8232649012	21.6206281128	28.1064837078
H	23.3144534346	20.5940989519	30.1731141045
H	24.1618010015	22.1517052580	30.3725882444
H	25.3828750452	19.6228436422	29.0948687547
H	25.5208084909	20.0452059891	30.8112839460
H	27.5600698923	20.6855703026	29.7999286100
H	26.6943600624	22.2041367346	30.1596627759
N	23.3281663044	27.3648268546	25.6457482356
C	23.5284288545	28.7336365724	25.2037317431
C	24.8650538847	29.3132162718	25.6993420800
C	26.1217253897	28.7916257860	24.9807256734
N	26.4533023773	27.4335404913	25.3737659323
H	22.7193765950	29.3428111567	25.6416895456
H	23.4604857852	28.8358329395	24.0993238663
H	24.9623183683	29.1231392129	26.7787331534
H	24.8291103382	30.4056616125	25.5621123601
H	26.9668703970	29.4361621109	25.2766985970
H	25.9950673713	28.8938615053	23.8814063769
C	26.7649691692	25.1187402928	24.7579604922
C	26.8995523252	24.6625780614	26.0847642761
H	26.9074289472	25.4014553785	26.8879764410
C	26.9471795550	23.2961515792	26.3696417465
C	26.8827569955	22.3712454138	25.3086724630
H	26.8819675277	21.3065004475	25.5486749674
C	26.7481594755	22.8060205626	23.9881594441
C	26.7020801478	24.1883235335	23.7187788756
H	26.5592355118	24.5112948030	22.6861336165
C	26.5543943265	26.5444639421	24.4606546673
H	26.4158014025	26.7901210611	23.3874724404
C	26.9267693906	22.8506564111	27.7722426664
H	26.9363851863	23.6636212845	28.5276880293
C	26.5233454319	21.8152099818	22.9238223428
H	26.5388017061	20.7545399732	23.2502330470
C	23.1931672999	23.2104869838	26.6960460662
C	23.1309231669	24.5773114249	26.4147035437
H	23.2319093989	25.3166232707	27.2112735161
C	23.0108414829	25.0358182803	25.0873758298
C	22.9328795180	24.1059701488	24.0487230221
H	22.8801582785	24.4320917802	23.0086048668
C	22.9964026198	22.7239574261	24.3149207089
C	23.1129049823	22.2869056470	25.6356401207
H	23.2041607608	21.2240441370	25.8662239091
C	23.4806219819	22.7682753699	28.0697164131
H	23.5676407832	23.5813381951	28.8202925254
C	23.1052679314	26.4680232172	24.7619312545
H	23.0425532773	26.7143247020	23.6818291115
C	23.0796204179	21.7397146760	23.2255281455
H	23.1679834818	20.6813306339	23.5472969232

CC-butane (structure with an internal void):

N	24.3558624743	27.9307686318	31.8766982091
C	23.7364215562	27.2332431232	32.9907834961
C	24.2486432357	25.7904593119	33.0972817896
C	23.8426377445	24.9158040923	31.9101293447
C	24.3352705203	23.4719279381	32.0581011877
N	23.8690670629	22.6457302656	30.9581323567
H	22.6280365912	27.2382959496	32.9240945827
H	24.0153512826	27.7731376076	33.9114625761
H	23.8601386832	25.3543050152	34.0326547308
H	25.3465931100	25.8145736843	33.1885816958
H	22.7457713313	24.9053423694	31.8018880366

H	24.2463146771	25.3411922248	30.9781339038
H	23.9199344777	23.0491004688	32.9898668455
H	25.4413777255	23.4592554962	32.1534111692
N	21.4245819236	31.1116194864	27.0430159038
C	20.6076355701	31.7547847682	26.0273096899
C	19.7771424452	30.7140156870	25.2665278717
C	18.8154627383	31.3479105094	24.2607568015
C	17.9544604643	30.3144235221	23.5212143499
N	18.7588830085	29.4913055545	22.6343339244
H	21.2156116057	32.3456833431	25.3110103486
H	19.9242544387	32.4544090448	26.5390217035
H	19.2152519388	30.1099488946	25.9974719449
H	20.4589336694	30.0228262002	24.7470000831
H	18.1420012059	32.0494116030	24.7804661005
H	19.3766801242	31.9356993819	23.5167671800
H	17.2230862966	30.8499994683	22.8930375659
H	17.3834667899	29.7055358707	24.2535912069
N	27.8881326577	30.8419996628	27.2889919572
C	29.3345318785	30.8586298510	27.1485694031
C	29.7552827800	30.4495936378	25.7324505645
C	31.2735395390	30.4781294676	25.5465498347
C	31.7174469811	30.0923751394	24.1279875509
N	31.3656827117	28.7128057218	23.8358275099
H	29.8364404236	30.2075707353	27.8948048658
H	29.6743844212	31.8930127320	27.3347628701
H	29.3749724714	29.4376876816	25.5233911938
H	29.2680752313	31.1236234787	25.0090525360
H	31.6608898452	31.4865692714	25.7686011628
H	31.7505192866	29.7885824992	26.2617113471
H	32.8156183344	30.1764150520	24.0675974116
H	31.2857567188	30.8006103232	23.3892979195
N	27.4379860659	19.1363736905	26.8586878842
C	28.4066328758	18.4197404055	26.0462691882
C	29.5852338627	19.3227949638	25.6609857935
C	29.1920316380	20.4865801939	24.7487023344
C	30.4046176346	21.3383501736	24.3580127088
N	30.0336305576	22.3929121814	23.4316524677
H	27.9477369184	17.9785071154	25.1361606389
H	28.7926423821	17.5867087248	26.6586584343
H	30.3479343341	18.7008184085	25.1628945103
H	30.0438899019	19.7109582332	26.5847848452
H	28.4470517357	21.1220535865	25.2525717678
H	28.7147283903	20.1088053568	23.8298276435
H	31.1372907283	20.6898656973	23.8446047459
H	30.8995296522	21.7340340648	25.2695717740
N	21.0127207479	19.3348311051	26.1799403333
C	19.5994968558	19.2413284832	25.8597102972
C	19.3309237672	19.6891879347	24.4164306769
C	19.5344422717	21.1890733130	24.1967747527
C	19.2439257167	21.5984863720	22.7490116197
N	19.2587147449	23.0417876778	22.5917304108
H	18.9681278711	19.8253990931	26.5622901172
H	19.3122504619	18.1807987994	25.9571300769
H	18.2943340510	19.4174917172	24.1564349038
H	19.9892491590	19.1145222409	23.7450582022
H	20.5657374936	21.4743035497	24.4572475244
H	18.8699863378	21.7630268194	24.8627906803
H	19.9515390137	21.0909450689	22.0609796837
H	18.2282458347	21.2524361825	22.4857446867
C	24.0930213612	29.2092142162	29.8384498599
C	23.1837878738	29.8134671858	28.9659606092
H	22.1080837009	29.7342784262	29.1343942449
C	23.6361035791	30.5394605010	27.8460686714
C	25.0093507834	30.6455009941	27.6103760464
H	25.3884208325	31.1983003076	26.7486307658
C	25.9397291663	30.0360483710	28.4755738350
C	25.4742940552	29.3226517328	29.5832514495

H	26.1704486980	28.8419625323	30.2730511175
C	23.5887679683	28.4702234282	31.0060230678
H	22.4847016397	28.4134273537	31.0929921811
C	22.6957744989	31.1789487257	26.9115956086
H	23.1650000002	31.7302913539	26.0702625413
C	27.3882217003	30.1379460521	28.2335329910
H	28.0290564760	29.5644501266	28.9349905168
C	24.4096529453	21.2040011224	29.0920620092
C	25.4316235076	20.5689957152	28.3824462462
H	26.4761926426	20.6904287596	28.6751629648
C	25.1380761793	19.7551148355	27.2703347945
C	23.8073043301	19.5884285750	26.8797948778
H	23.5481565030	18.9636230086	26.0231616560
C	22.7643849704	20.2204110604	27.5861353556
C	23.0726455227	21.0233313752	28.6863818538
H	22.2865122605	21.5298988225	29.2497602288
C	24.7507195854	22.0540263796	30.2438421871
H	25.8354884641	22.1509496651	30.4588526420
C	26.2062214228	19.0793010431	26.5173809117
H	25.8747544166	18.5044411941	25.6285817922
C	21.3603432000	20.0526952035	27.1801151609
H	20.6138193683	20.5902309714	27.7997579952
N	27.6750420683	26.4850825521	19.0071369287
C	26.8067195601	26.1771178759	17.8837026389
C	25.4237377912	26.8161065389	18.0663805628
C	24.5041933814	26.5607044116	16.8703017131
C	23.1105357538	27.1773287267	17.0361879121
N	22.3784631970	26.5588323177	18.1305291570
H	26.6921196532	25.0835826663	17.7302977315
H	27.2756759152	26.5931400157	16.9751801049
H	25.5474765064	27.8990168237	18.2300284021
H	24.9602293452	26.4116872193	18.9800946871
H	24.3903616907	25.4760375351	16.7119807436
H	24.9578687835	26.9718085156	15.9531022201
H	22.5331340395	26.9901519052	16.1145336967
H	23.1913369609	28.2782526716	17.1571927916
C	20.9782380330	26.8249887019	20.0864051209
C	20.2849642470	27.7326636980	20.8915633445
H	20.3414949945	28.8060156993	20.7008335348
C	19.4840028432	27.2823029449	21.9599763760
C	19.3963083680	25.9122514521	22.2177554695
H	18.7861279646	25.5347630993	23.0404481190
C	20.0948830957	24.9838841718	21.4209704771
C	20.8776957700	25.4460334544	20.3600137663
H	21.4198445804	24.7481048567	19.7193304374
C	21.7844373140	27.3283189533	18.9627606338
H	21.8354348168	28.4327753497	18.8717444101
C	18.7289069690	28.2229650454	22.8027011902
H	18.1129916366	27.7581057574	23.5993045261
C	20.0079246209	23.5378631107	21.6811658281
H	20.6326275999	22.8967221681	21.0257445762
C	28.9177923242	25.6976352478	20.9247744511
C	29.2541627182	24.5908512311	21.7078735884
H	28.9087275562	23.5899115674	21.4423408829
C	30.0333941093	24.7439805574	22.8717937497
C	30.4829138415	26.0167290501	23.2308623593
H	31.0878534338	26.1646760399	24.1272236778
C	30.1635756790	27.1415237818	22.4448492774
C	29.3786334259	26.9753297281	21.3011769796
H	29.1024761081	27.8299914391	20.6807657204
C	28.0716064182	25.5109780256	19.7357460172
H	27.7871762124	24.4614647370	19.5124128506
C	30.3652882432	23.5930368095	23.7253124051
H	30.9230312311	23.8329683920	24.6539037267
C	30.6219891417	28.4878628750	22.8190623483
H	30.2716676606	29.3108342496	22.1629829868

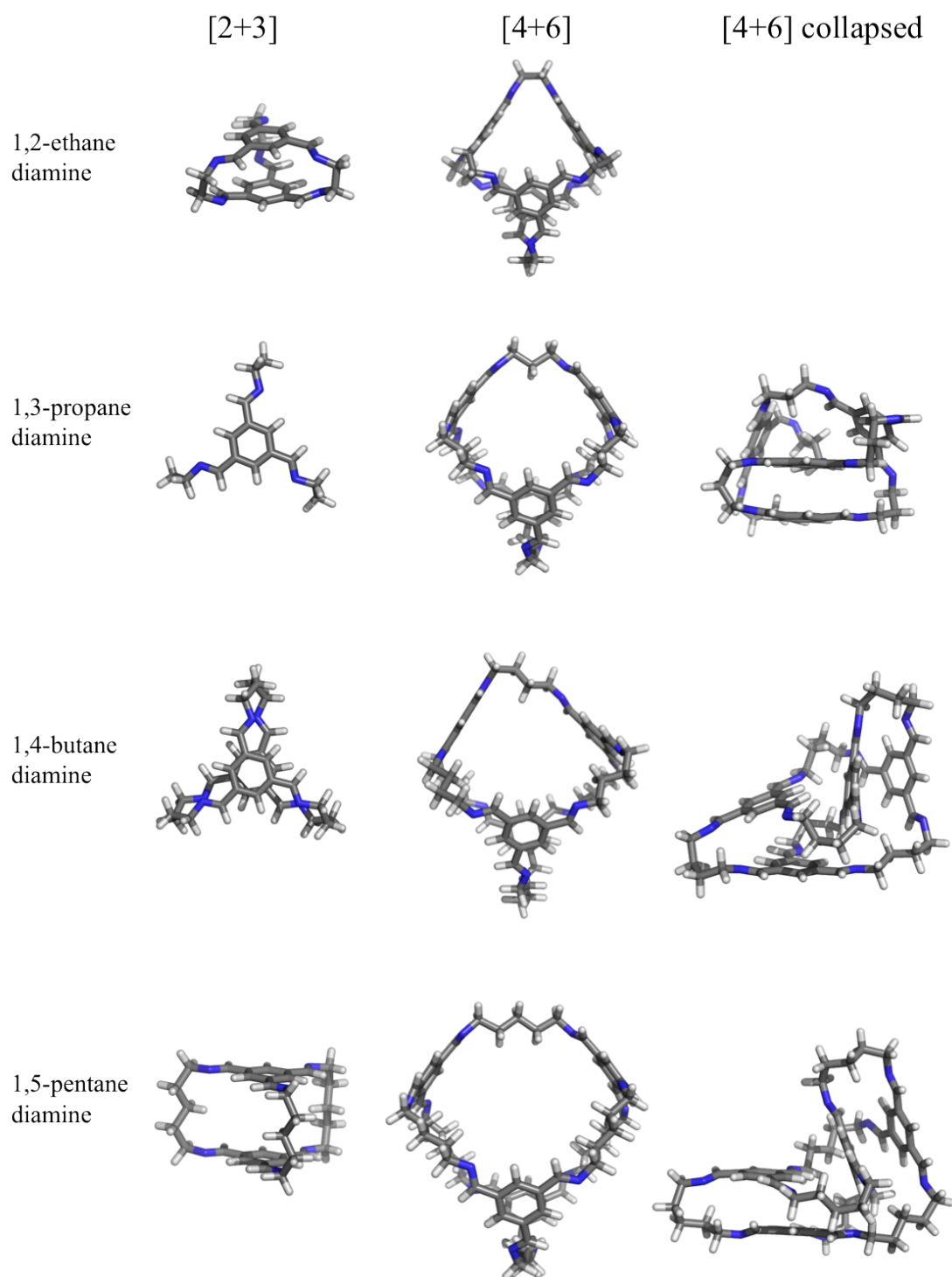


Figure S9. Calculated structures of the lowest energy conformer for both the [2+3] and [4+6] cages formed from reaction of each alkanediamine with 1,3,5-triformyl benzene. If a collapsed [4+6] structure was found, this is also shown.

4. References

- (1) Lydon, D. P.; Campbell, N. L.; Adams, D. J.; Cooper, A. I. *Synth. Commun.* **2011**, *41*, 2146.
- (2) Bruker (2009). SAINT V7.68a, BRUKER AXS Inc., Madison, WI, USA.
- (3) Bruker (2008). SADABS V2008-1, BRUKER AXS Inc., Madison, WI, USA.
- (4) Barbour, L. J. *J. Supramolecular Chem.* **2001**, *1*, 189.
- (5) Sheldrick, G. M. *Acta Cryst. A* **2008**, *64*, 112.
- (6) Spek, A. L. *J. Appl. Cryst.* **2003**, *36*, 7.
- (7) Robeson, L. M. *J. Membrane Sci.* **1991**, *62*, 165.
- (8) Kolossvary, I.; Guida, W. *J. Am. Chem. Soc.* **1996**, *118*, 5011.
- (9) Jelfs, K. E.; Schiffmann, F.; Jones, J. T. A.; Slater, B.; Cora, F.; Cooper, A. I. *Phys. Chem. Chem. Phys.* **2011**, *13*, 20081.
- (10) Van de Vondele, J.; Krack, M.; Mohamed, F.; Parrinello, M.; Chassaing, T.; Hutter, J. *Comput. Phys. Commun.* **2005**, *167*, 103.
- (11) Perdew, J.; Burke, K.; Ernzerhof, M. *Phys. Rev. Lett.* **1996**, *77*, 3865.
- (12) Van de Vondele, J.; Hutter, J. *J. Chem. Phys.* **2007**, *127*, 114105.
- (13) Goedecker, S.; Teter, M.; Hutter, J. *Phys. Rev. B* **1996**, *54*, 1.
- (14) Grimme, S.; Antony, J.; Ehrlich, S.; Krieg, H. *J. Chem. Phys.* **2010**, *132*, 154104.
- (15) Jones, J. T. A.; Hasell, T.; Wu, X.; Bacsá, J.; Jelfs, K. E.; Schmidtman, M.; Chong, S. Y.; Adams, D. J.; Trewin, A.; Schiffman, F.; Cora, F.; Slater, B.; Steiner, A.; Day, G. M.; Cooper, A. I. *Nature* **2011**, *474*, 367.
- (16) Hasell, T.; Chong, S. Y.; Jelfs, K. E.; Adams, D. J.; Cooper, A. I. *J. Am. Chem. Soc.* **2012**, *134*, 588.
- (17) Rappe, A.; Casewit, C. J.; Colwell, K. S.; Goddard, W., III; Skiff, W. M. *J. Am. Chem. Soc.* **1992**, *114*, 10024.
- (18) Sun, H. *Macromolecules* **1995**, *28*, 701.
- (19) Jorgensen, W. L.; Maxwell, D.; TiradoRives, J. *J. Am. Chem. Soc.* **1996**, *118*, 11225.
- (20) Tozawa, T.; Jones, J. T. A.; Swamy, S. I.; Jiang, S.; Adams, D. J.; Shakespeare, S.; Clowes, R.; Bradshaw, D.; Hasell, T.; Chong, S. Y.; Tang, C.; Thompson, S.; Parker, J.; Trewin, A.; Bacsá, J.; Slawin, A. M. Z.; Steiner, A.; Cooper, A. I. *Nat Mater* **2009**, *8*, 973.
- (21) Mitra, T.; Wu, X.; Clowes, R.; Jones, J. T. A.; Jelfs, K. E.; Adams, D. J.; Trewin, A.; Bacsá, J.; Steiner, A.; Cooper, A. I. *Chem.-Eur. J.* **2011**, *17*, 10235.
- (22) Bojdys, M. J.; Briggs, M. E.; Jones, J. T. A.; Adams, D. J.; Chong, S. Y.; Schmidtman, M.; Cooper, A. I. *J. Am. Chem. Soc.* **2011**, *133*, 16566.
- (23) Jelfs, K. E.; Wu, X.; Schmidtman, M.; Jones, J. T. A.; Warren, J. E.; Adams, D. J.; Cooper, A. I. *Angew. Chem. Int. Ed.* **2011**, *50*, 10653.
- (24) Jones, J. T. A.; Holden, D.; Mitra, T.; Hasell, T.; Adams, D. J.; Jelfs, K. E.; Trewin, A.; Willock, D. J.; Day, G. M.; Bacsá, J.; Steiner, A.; Cooper, A. I. *Angew. Chem. Int. Ed.* **2011**, *50*, 749.